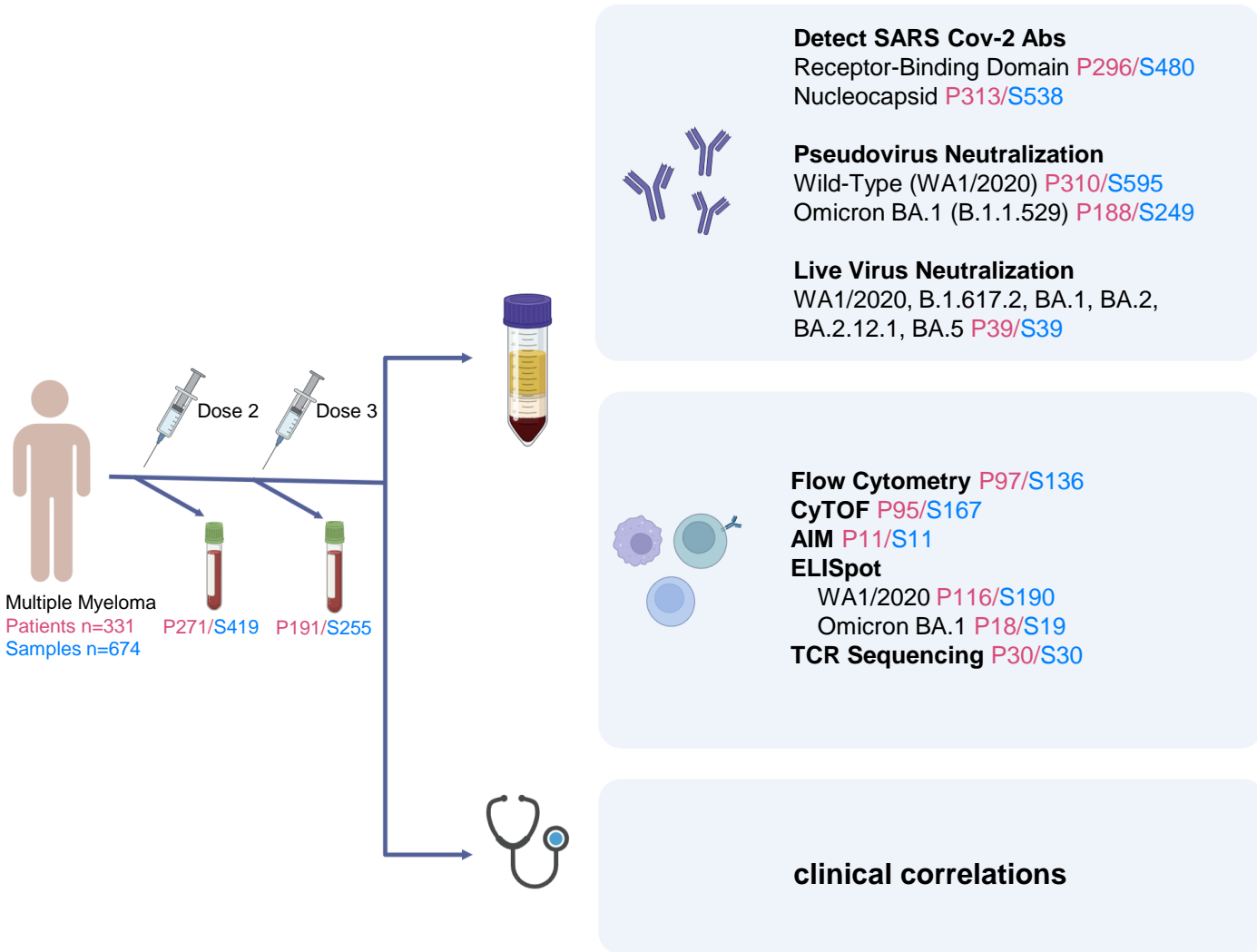


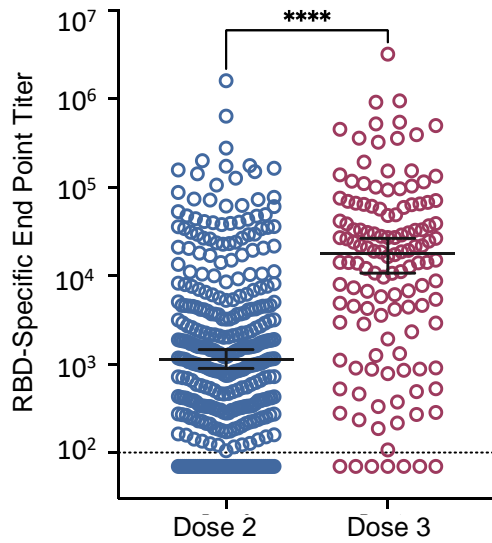
## Supplementary Figure 1



### Supplementary Fig 1. Overall Strategy.

Figure shows time points for sample collection, assays performed as well as the number of patients studied. (Patients:P, Samples:S). Plasma collected from these time points was used to perform serologic testing for response against WA and BA variants using RBD ELISA, Pseudovirus neutralization and live virus neutralization assays. Mononuclear cells isolated from the blood were examined for RBD specific B cells and T cell responses against both WA and BA variants using flowcytometry, single cell mass cytometry, activation induced marker expression (AIM) assay) as well as interferon gamma specific ELISpot assay for WA and BA spike protein. In addition TCR sequencing analysis via T-Detect assay (adaptive) was performed to identify SARS-CoV-2 specific T cells. Immune repertoire analysis was performed using CyTOF. Detailed clinical data was obtained and used for clinical correlations with the various assays.

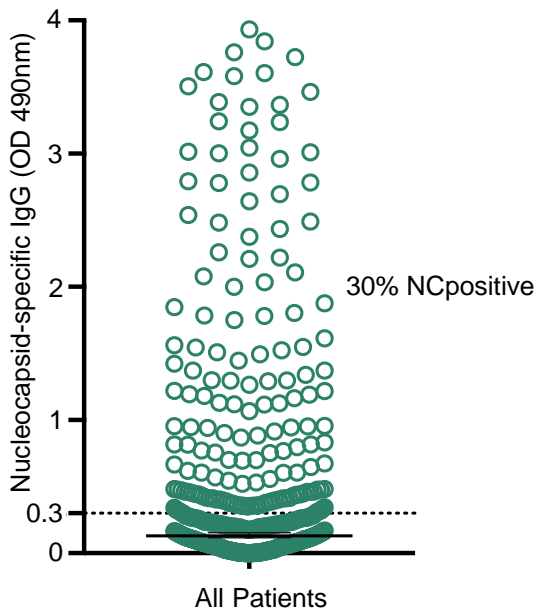
## Supplementary Figure 2



### Supplementary Fig 2.

Plasma obtained from myeloma patients following 2 or 3 doses of SARS-CoV-2 vaccines were analyzed for RBD-specific antibodies. RBD-specific end point titer collected after dose 2 (n=352) and after dose 3 (n=128) vaccine. Bar represents median with 95% CI (\*\*\*\* $p < 0.0001$ , Mann Whitney).

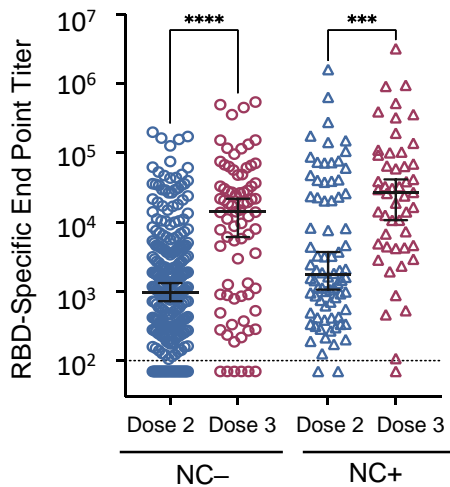
### Supplementary Figure 3



### Supplementary Fig 3.

Environmental exposure of SARS-CoV-2 infection was monitored by measuring nucleocapsid (NC) antibodies in the plasma by ELISA (n=538). Nucleocapsid positive (NC+) patients were identified with OD >0.3. Dotted line shows upper limit of negativity. NC reactivity in the cohort was 30%.

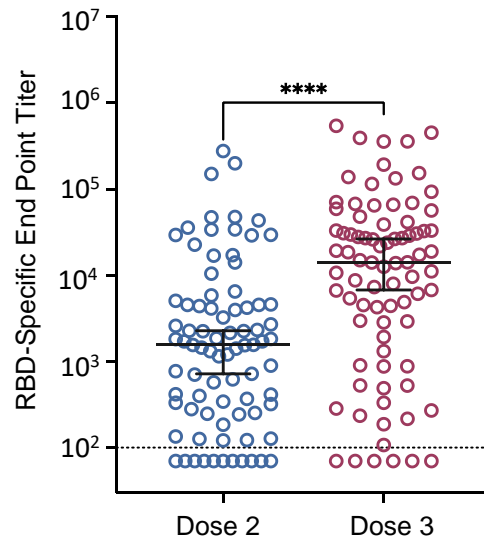
## Supplementary Figure 4



### Supplementary Fig 4.

RBD reactivity in nucleocapsid positive and negative patients. (NC-: Dose 2, n=273; Dose 3, n=78) and NC positive (Dose 2, n=78; Dose 3, n=50). Bar represents median with 95% CI. Dotted line at  $10^2$  is the cutoff for negative titer (\*\*p<0.001, \*\*\*\*p<0.0001, Kruskal Wallis).

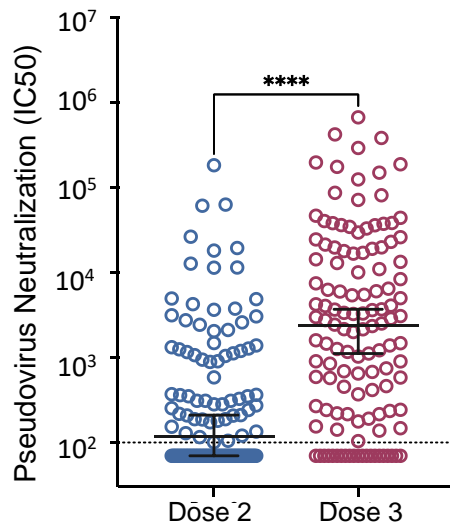
## Supplementary Figure 5



### Supplementary Fig 5.

Measurement of RBD-specific endpoint titer in 82 paired dose 2 and dose 3 samples analyzed. Bar represents median with 95% CI (\*\*\*\* $p < 0.0001$ , Wilcoxon test).

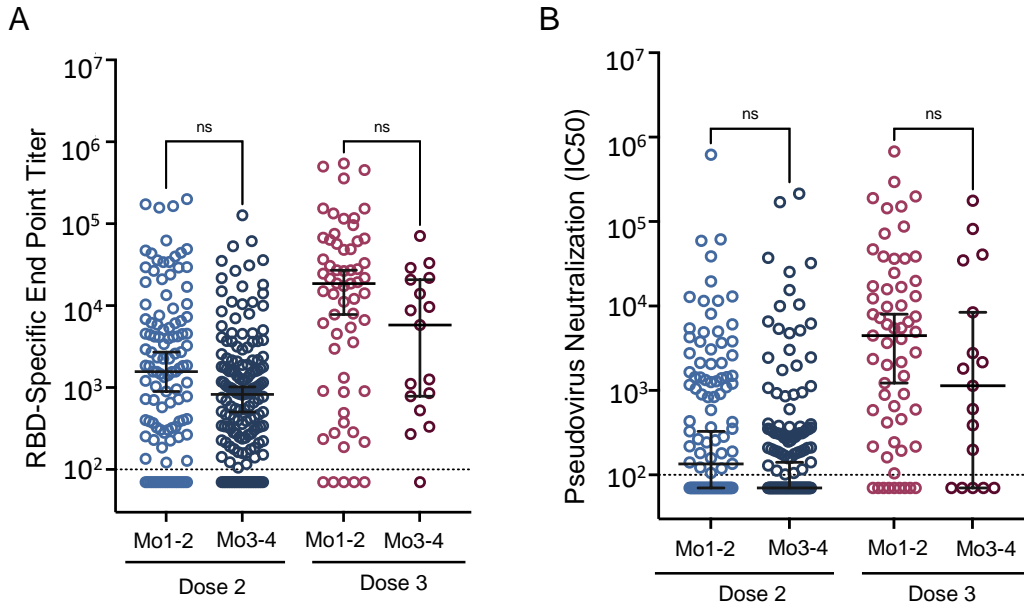
## Supplementary Figure 6



### Supplementary Fig 6.

Pseudovirus neutralization (IC<sub>50</sub>) was measured in 124 paired samples analyzed after dose 2 and after dose 3 vaccine. Bar represents median with 95% CI (\*\*\*\* $p < 0.0001$ , Wilcoxon test).

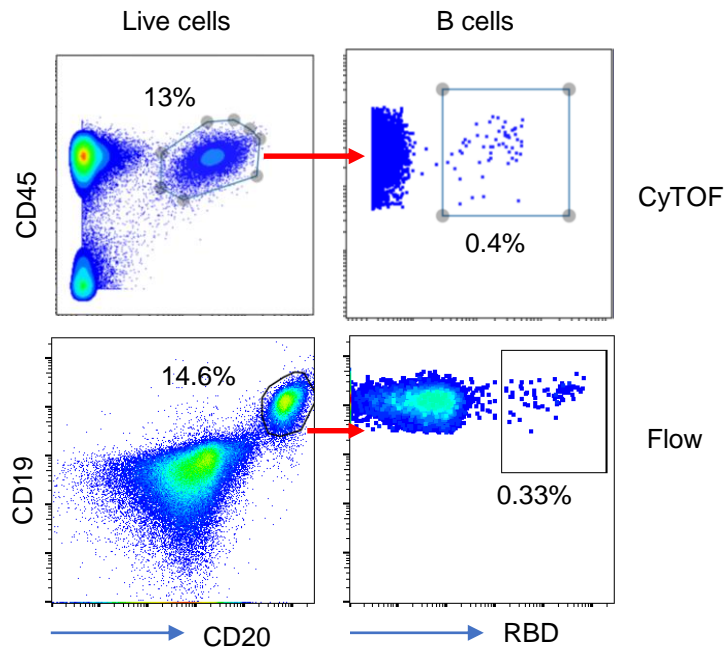
## Supplementary Figure 7



### Supplementary Fig 7.

Persistence of RBD-specific and pseudovirus neutralizing antibodies. A. RBD-specific end point titer measured after dose 2 at month 1-2 (n=115) and month 3-4 (n=158), as well as after dose 3 (month 1-2, n=61; month 3-4, n=17). B. Pseudovirus neutralization titer measured after dose 2 at month 1-2 (n=115) and month 3-4 (n=158), and after dose 3 at month 1-2 (n=61) and month 3-4 (n=17). Bar represents median with 95% CI (ns: not significant, Kruskal Wallis).

## Supplementary Figure 8

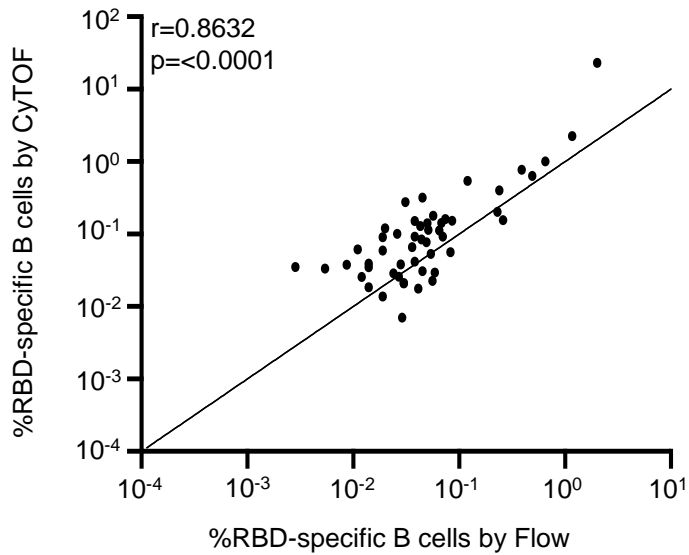


### Supplementary Fig 8.

Identification of RBD specific B cells. RBD specific B cells could be identified by both flow cytometry or CyTOF. Figure shows identification of RBD+B cells by CyTOF and flow cytometry on the same sample.



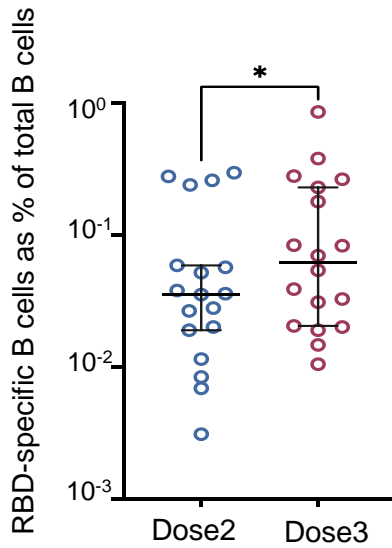
## Supplementary Figure 9



### Supplementary Fig 9.

Correlation between RBD-specific B cells as percent of total B cells measured by flow cytometry (x-axis) versus RBD-specific B cells as percent of total B cells measured by single cell mass cytometry (y-axis). The Pearson correlation (R) value is shown as well as the P-value of correlation.

## Supplementary Figure 10

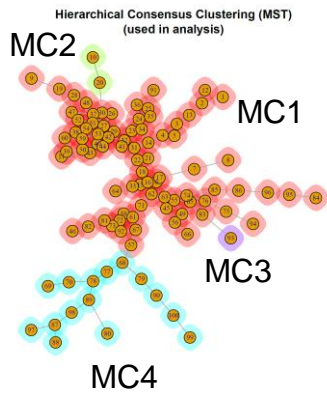


### Supplementary Fig 10.

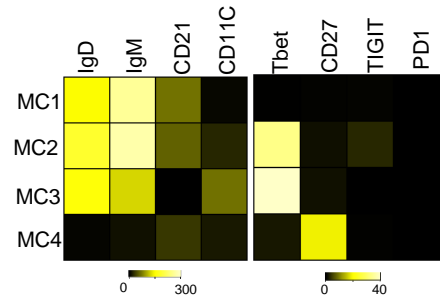
Proportions of RBD specific B cells (% of total B cells) in 18 paired dose 2 and dose 3 samples. Bar represents median with 95% CI (\* $p < 0.05$ , Wilcoxon test).

# Supplementary Figure 11

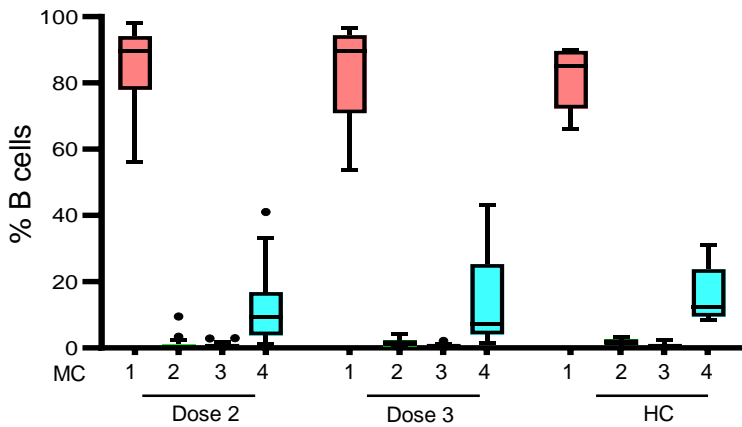
A



B



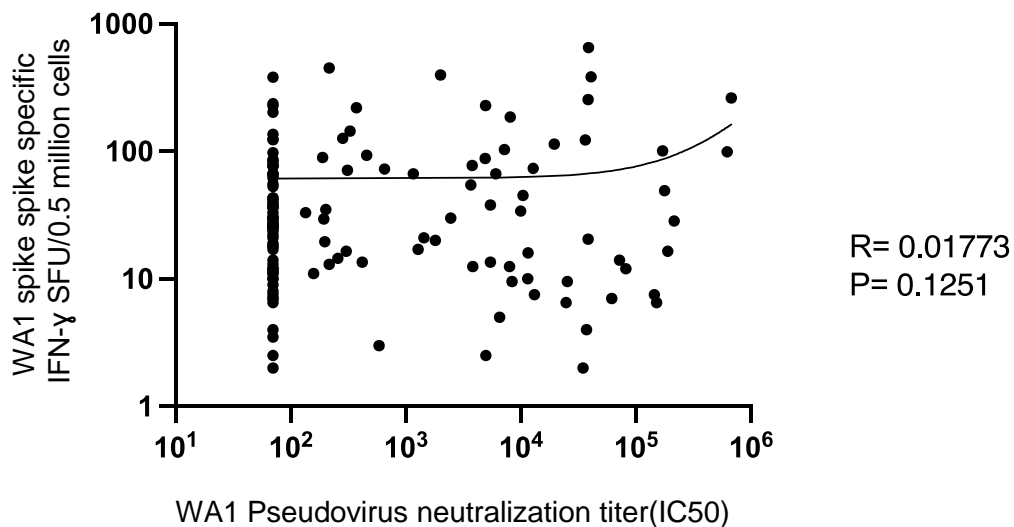
C



## Supplementary Fig 11.

FlowSOM of all B cells patients following vaccine Dose2 (D2:n=26), vaccine Dose 3 (D3:n=19) and healthy controls (HC, n=7) following SARS-CoV-2 vaccine. Panel A. shows clustering map with 4 distinct metaclusters (MC). Panel B is the heatmap of marker expression in these clusters. C. Bar graph shows proportions of B cells within the different clusters. Most B cells from patients following D2 and 3 of vaccines are naïve B cells (MC1). The distribution of B cells within these clusters is similar in patients and the healthy donors(HC).

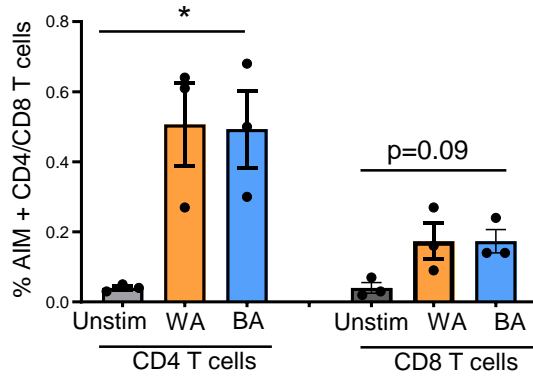
Supplementary Figure 12



**Supplementary Fig 12.**

WA1 spike specific T cells were detected using interferon gamma ELISpot. Plasma from the same time point was analyzed for WA1 reactivity using pseudovirus neutralization assay. Figure shows correlation between WA1 spike specific T cells and WA1 pseudo-virus neutralization titer.

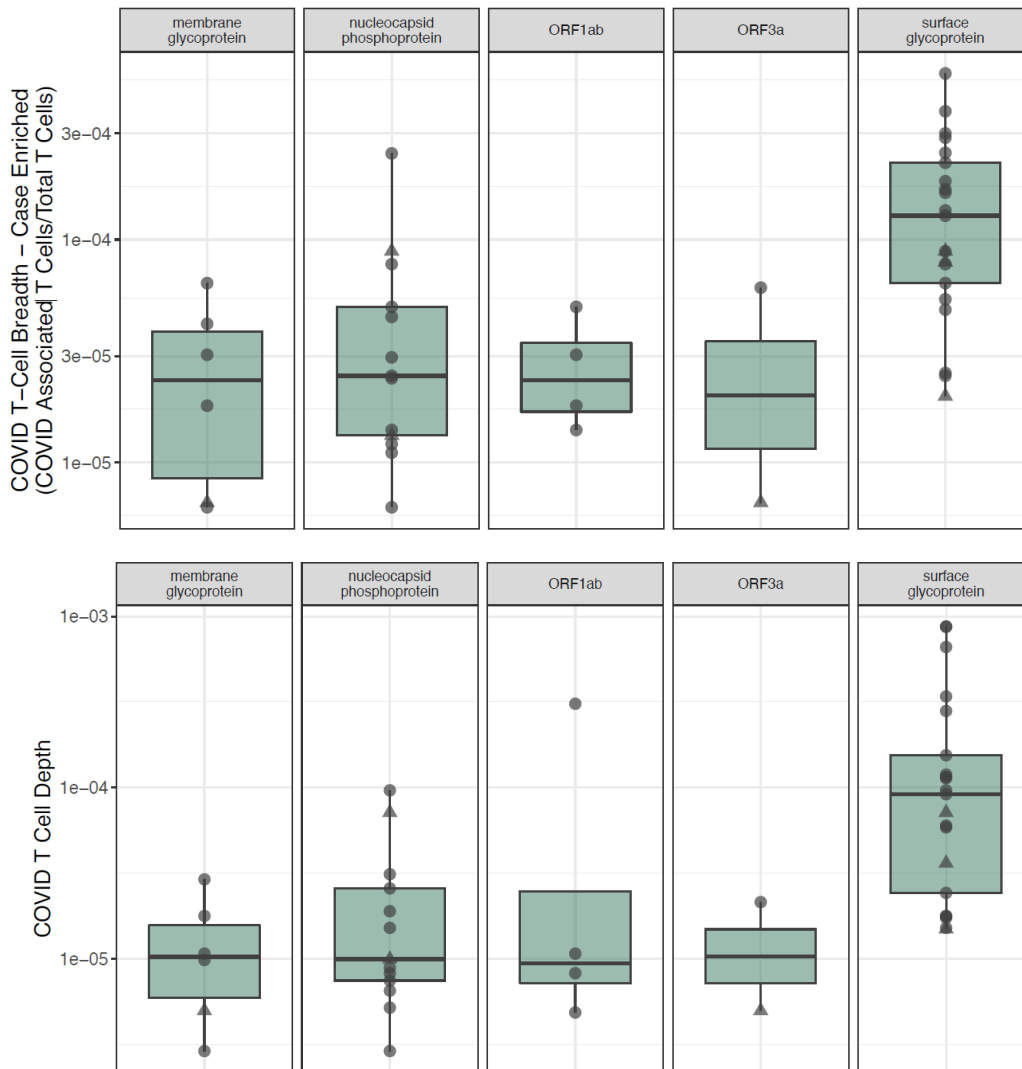
## Supplementary Figure 13



### Supplementary Fig 13.

WA and BA Spike-specific T cells as detected by AIM assay in healthy donors using CyTOF. Figure shows AIM+ CD4 and CD8 T cells in 3 healthy controls following SARS-CoV-2 vaccination. Bar graph shows mean $\pm$  SEM. \* $p < 0.05$  using one way Anova with Geisser Greenhouse correction.

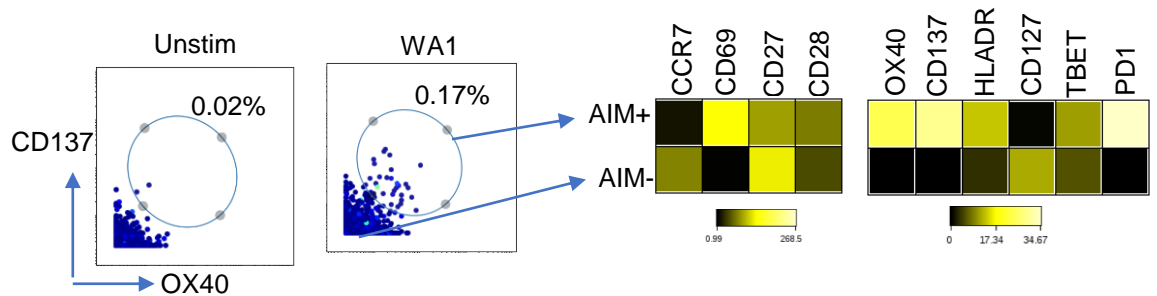
## Supplementary Figure 14



### Supplementary Fig 14.

T cell breath and depth against different regions of SARS-CoV-2 as analyzed by Adaptive Biotechnologies T-Detect assay for SARS CoV-2-specific T cells. COVID specific TCR breath is defined as the number of COVID-associated rearrangements out of the total number of rearrangements. TCR depth is defined as number of COVID-associated T cells (or templates) out of the total number of T cells (templates) in a sample. Panel on top shows that TCR breath within the surface glycoprotein is higher than against membrane or nucleocapsid phosphoprotein as well as other SARS-CoV-2 open reading frames (ORFs) consistent with vaccination targeting spike region. Panel 2 shows that similarly TCR depth within surface glycoprotein is higher than other ORFs again suggesting vaccination targeting spike region.

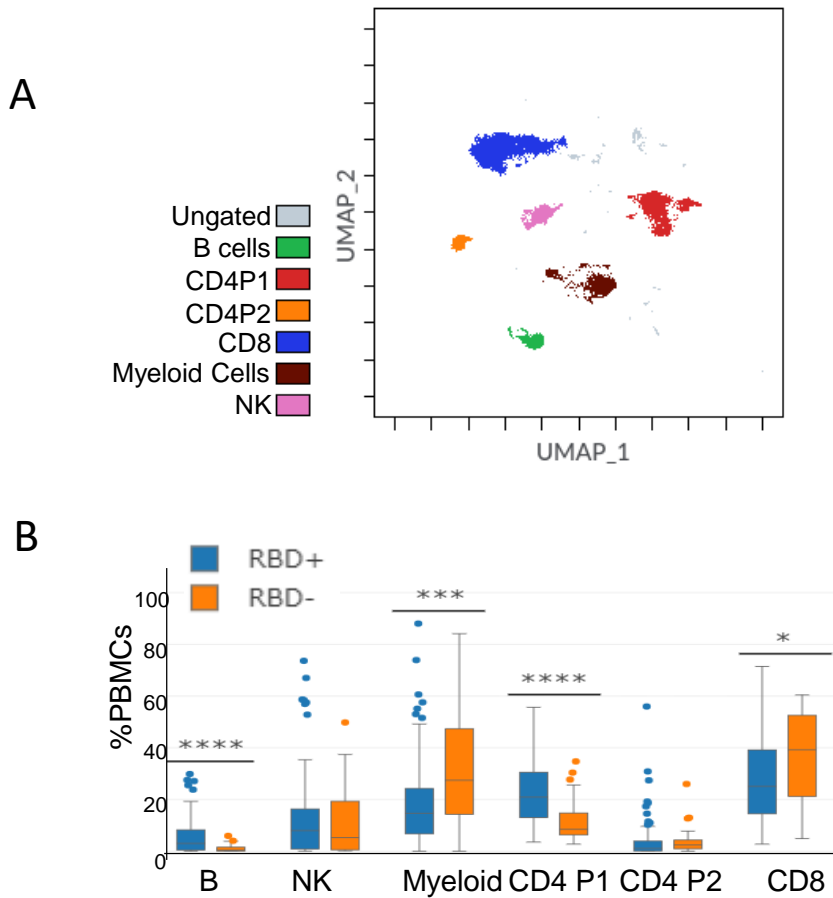
## Supplementary Figure 15



### Supplementary Fig 15.

Phenotype of AIM+ cells. PBMCs were cultured alone (Unstim) or stimulated with SARS-Cov-2 spike peptide (WA1) and analyzed using single cell mass cytometry. WA1 Spike specific CD4 T cells (AIM+) were identified based on upregulation of surface CD137 and OX40 as previously described. Heatmap shows difference in phenotype of AIM+ and AIM- CD4 T cells.

Supplementary Figure 16

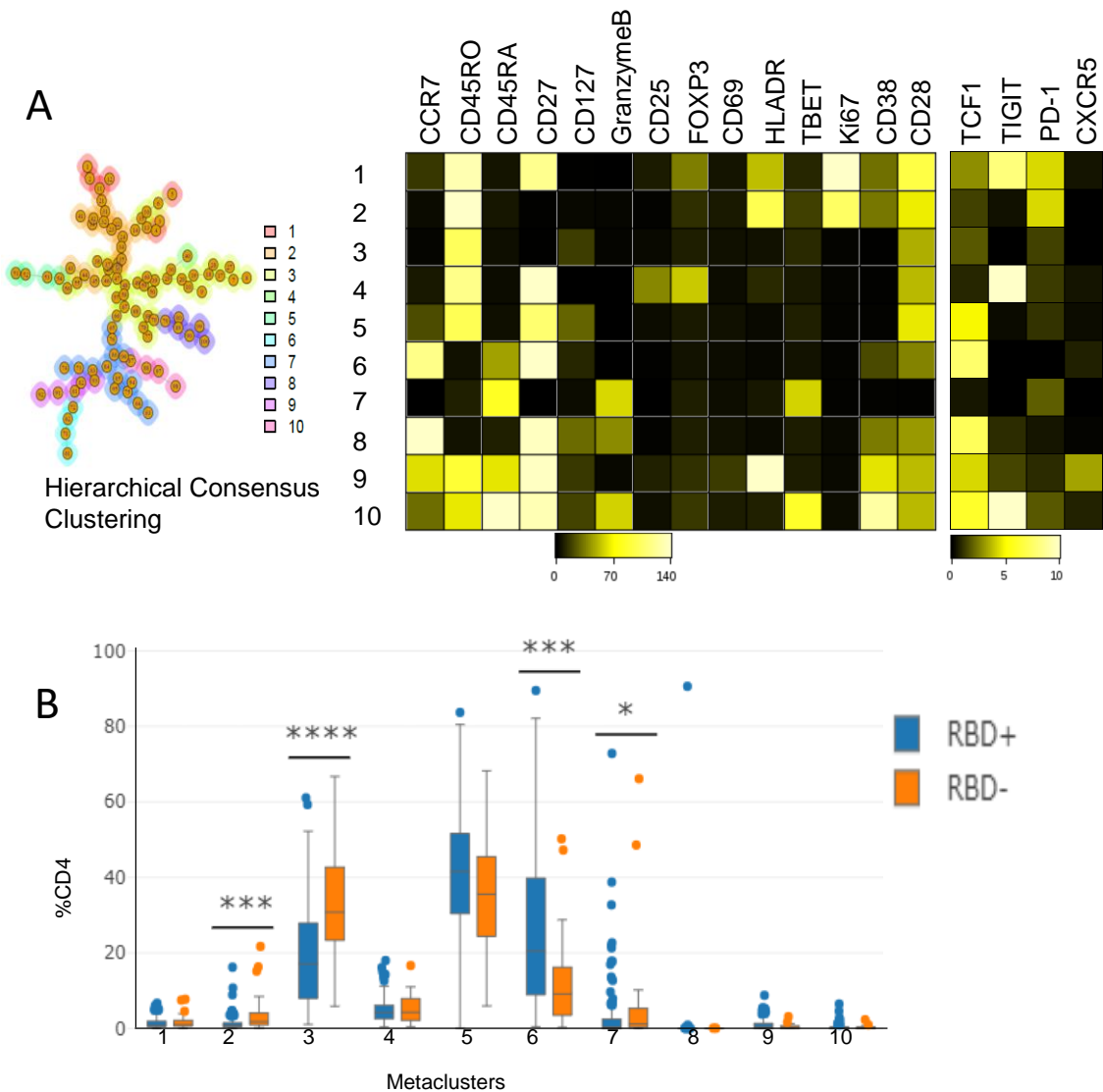


**Supplementary Fig 16.**

CytoTOF analysis was performed using 37 markers including cell surface phenotype markers and intracellular transcription factors and lytic molecules. A. UMAP clustering analysis performed using 6.9 million live/CD45+ peripheral blood mononuclear cells revealed 6 distinct cell clusters including B cell, NK and myeloid and CD8 cluster as well as 2 CD4 clusters. Cells not identified by the panel markers are labeled as ungated. B. Bar graph shows distribution of cell types in RBD+ (n=137) and RBD- (n=29) patient cohorts. \*p<0.05, \*\*\* p<0.001, \*\*\*\*p<0.0001 using Mann Whitney test.



Supplementary Figure 17



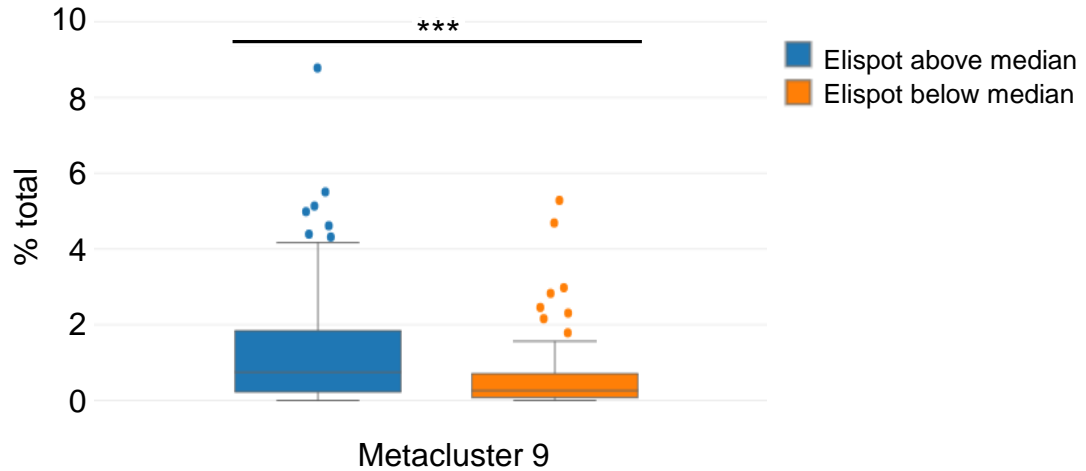
**Supplementary Fig 17.**

Correlation between CD4 immunophenotypes and vaccine response. CD4 T cell FlowSOM clustering analysis was performed using equal numbers of cells from each of the 172 samples using 20 different T cell specific cell surface phenotype markers, intracellular transcription factors and lytic molecules. 10 distinct clusters could be identified.

A. Clustering and heat map shows characteristics of these clusters.

B. Bar graph shows distribution of cells from RBD+ patients (n=134) and patients who are RBD- (n=28) following vaccination. (\*p<0.05, \*\*\*p<0.001, \*\*\*\*p<0.0001, Mann Whitney).

## Supplementary Figure 18



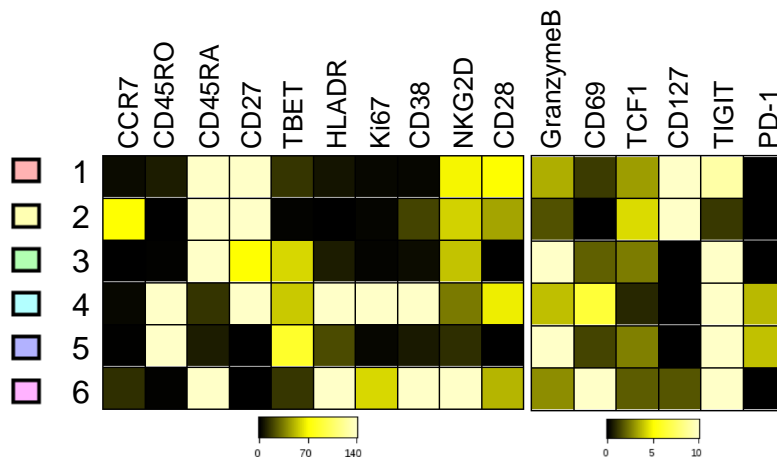
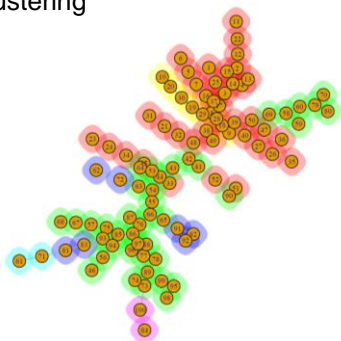
### Supplementary Fig 18.

Correlation between CD4+ T cell metacluster and ELISpot reactivity. Only metacluster 9 was significantly different in these cohorts. As noted in Suppl Fig 17, this is the only metacluster with CXCR5+ phenotype. (\*\*\*) $p < 0.001$ , Mann Whitney).

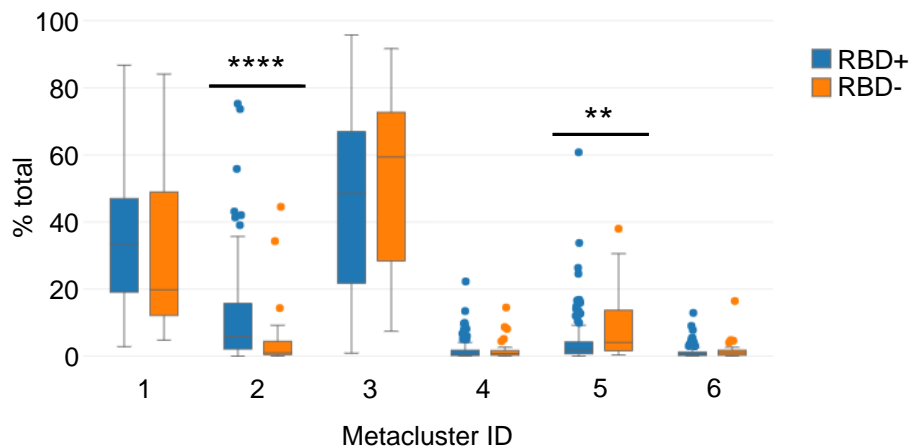
Supplementary Figure 19

A

Hierarchical Consensus Clustering



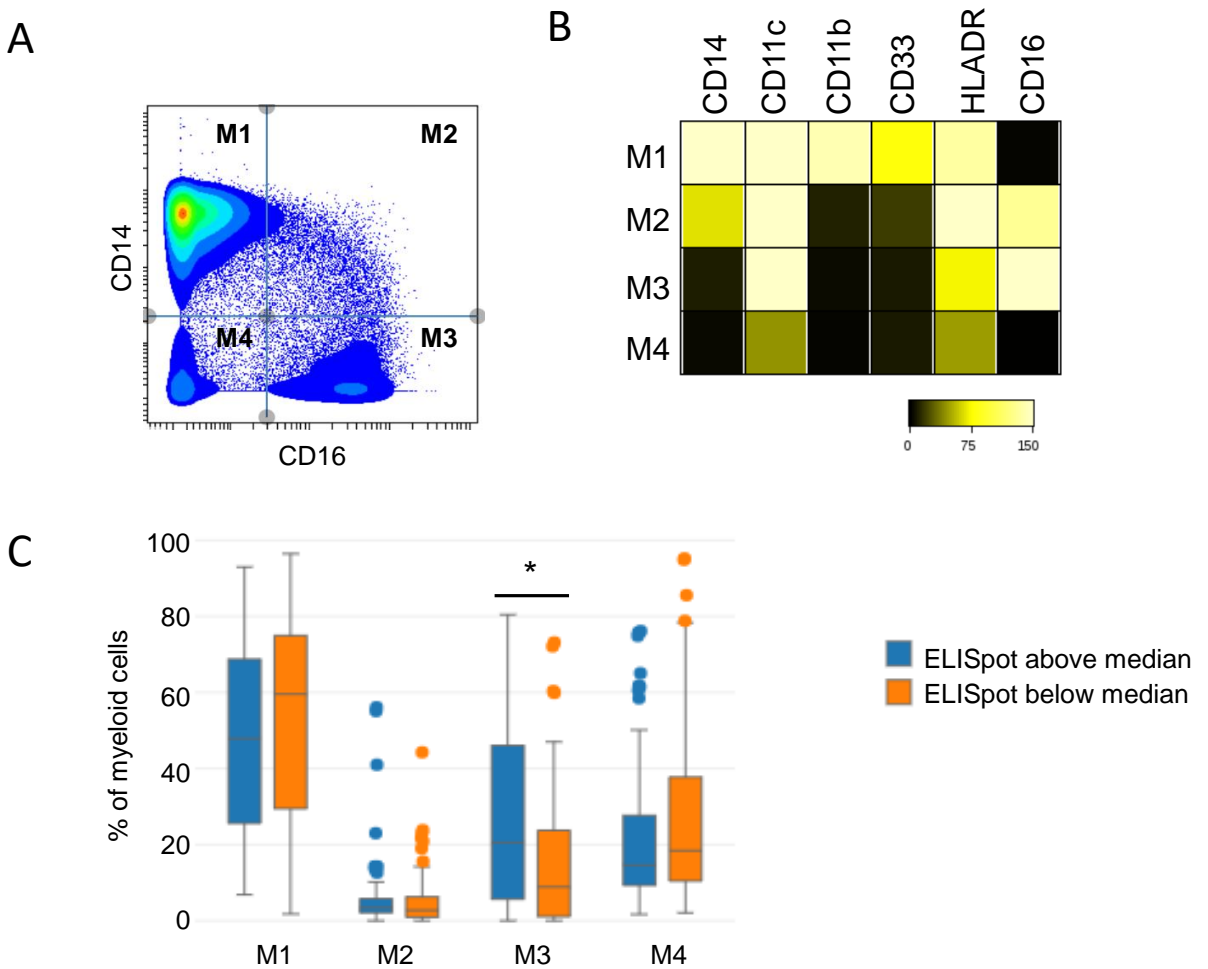
B



**Supplementary Fig 19.**

Correlation between CD8 immunophenotypes and vaccine response. Panel A shows CD8 T cell FlowSOM clustering map and expression of markers that define the 6 CD8 populations. Panel B: Bar graph shows distribution of cells from RBD+ (n=132) patients and patients who are RBD- (n=29) following vaccination. (\*\*p<0.01, \*\*\*\*p<0.0001, Mann Whitney).

Supplementary Figure 20



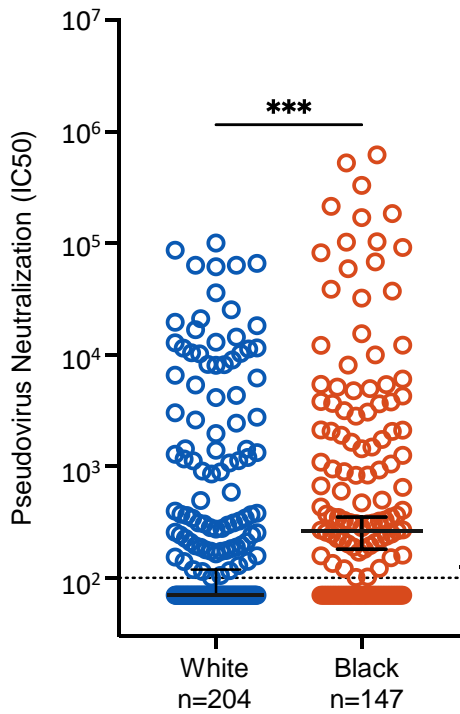
**Supplementary Fig 20.**

Correlation between myeloid immunophenotypes and vaccine response. PBMCs were analyzed using single cell mass cytometry. A. Dot plot shows gating strategy for myeloid cells (CD3/CD20/CD56 negative PBMCs).

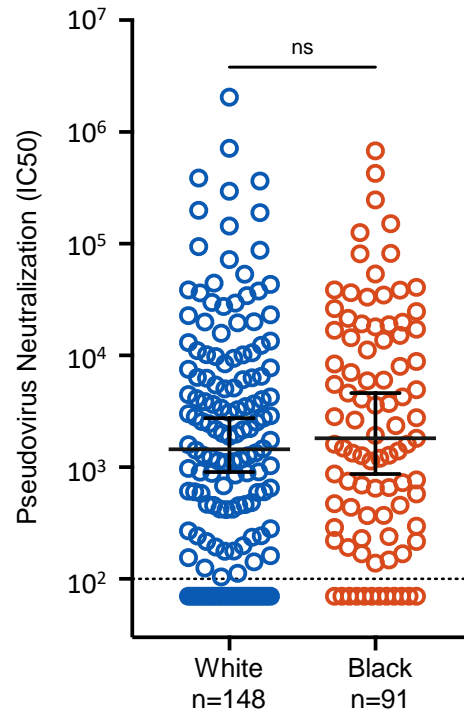
B. Heatmap shows expression of myeloid markers for the 4 groups of myeloid cells. C. Bar graph shows proportions of cells in the different myeloid populations based on WA spike specific IFN $\gamma$  ELISpot response. (\* $p < 0.05$ , Mann Whitney).

# Supplementary Figure 21

Dose 2



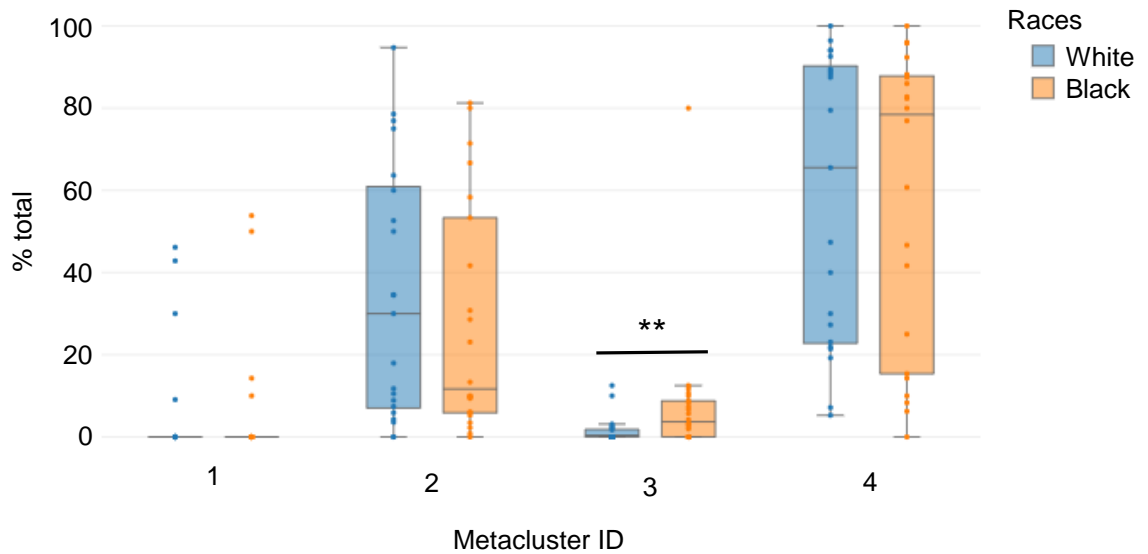
Dose 3



## Supplementary Fig 21.

nAb titers by race comparing Black or non-Black patients. Data shown for dose 2 and dose 3. Plots show median with 95% CI, (\*\*\*) $p < 0.001$ , Mann Whitney).

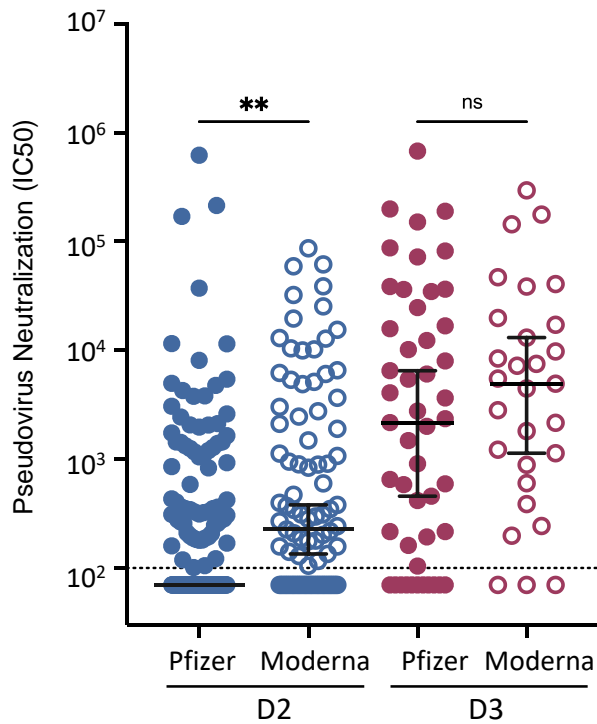
## Supplementary Figure 22



### Supplementary Fig 22.

Phenotype of RBD-specific B cells by race comparing Black or non-Black patients. FlowSOM clustering map and heatmap in main Fig1G. (\*\*p<0.01, Mann Whitney).

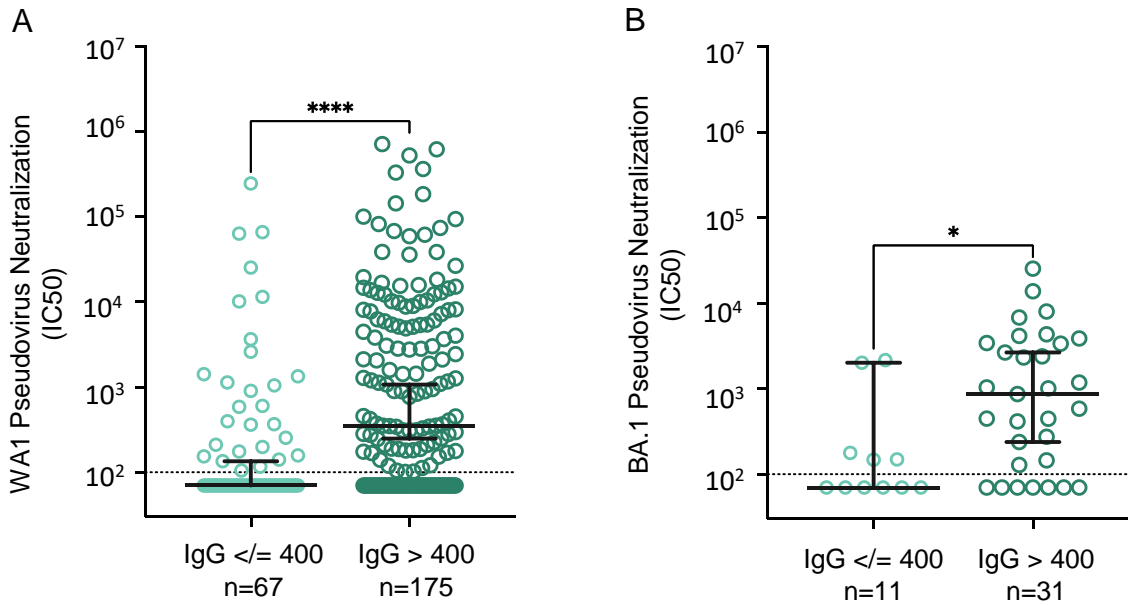
## Supplementary Figure 23



### Supplementary Fig 23.

nAb titers by vaccine type. Data are shown for dose 2 (Pfizer:n=183, Moderna:n=93) and dose 3 (Pfizer:n=49, Moderna:n=29) in NC negative patients. (\*\*p<0.01, Kruskal Wallis).

Supplementary Figure 24



### Supplementary Fig 24

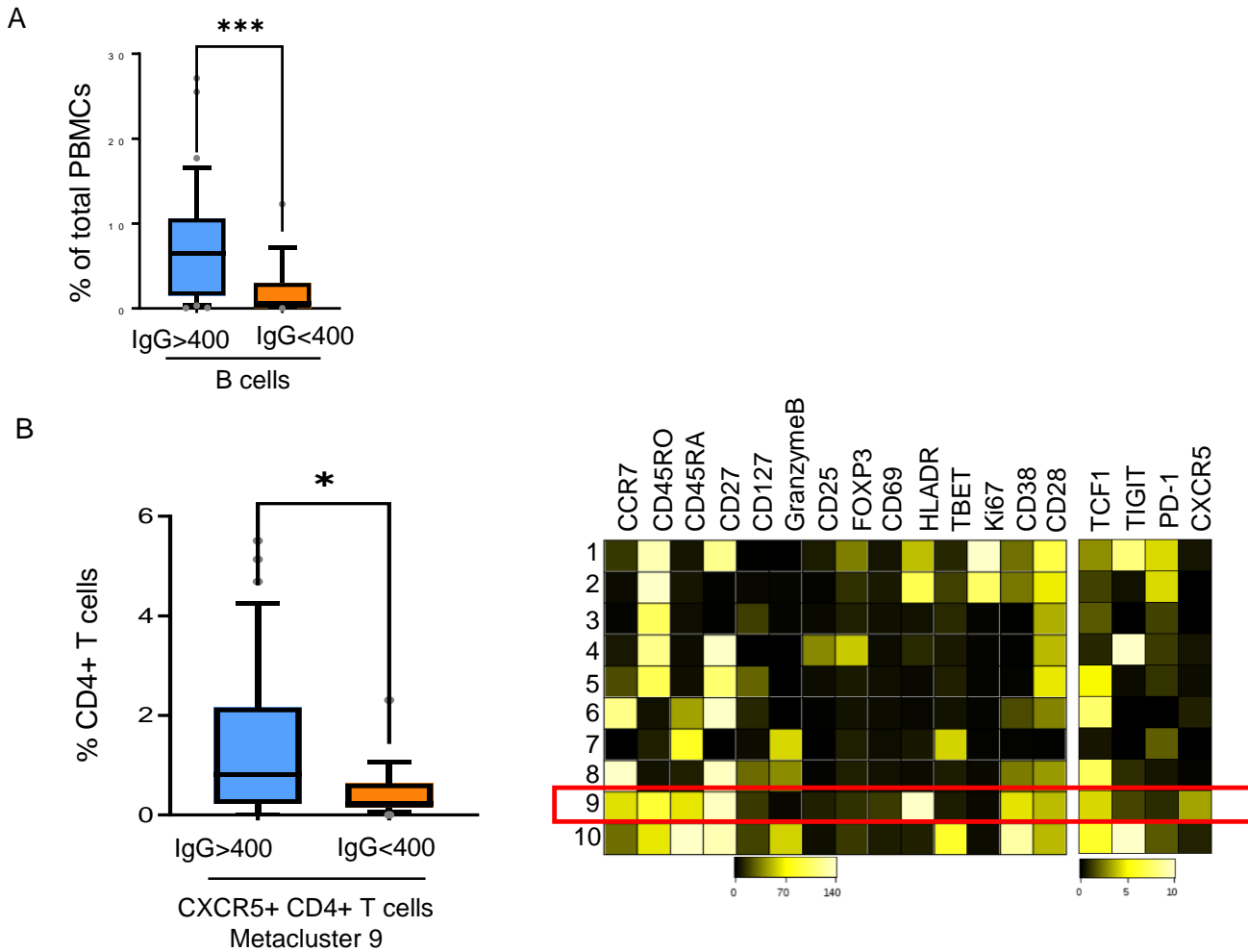
nAbs in MM patients with hypogammaglobulinemia.

A. Pseudovirus neutralizing antibodies against WA1 in patients with serum IgG  $\leq$  400 mg/dl vs those with IgG > 400 mg/dl. B. Pseudovirus neutralizing antibodies against BA1 in patients with serum IgG  $\leq$  400 mg/dl vs those with IgG > 400 mg/dl. Figure shows median with 95% CI. (\* $p < 0.05$ . \*\*\*\* $p < 0.0001$ . Mann-Whitney)

In case of IgG myeloma, only patients with VGPR or better were included to avoid artifact of clonal Ig on total Ig level.



Supplementary Figure 25



**Supplementary Fig 25**

Hypogammaglobulinemia and B/T cell phenotypes in MM.

Differences in characteristics and proportions of immune cells in patients with IgG>400 (n=36) or IgG<400 (n=17). A. Proportions of B cells in peripheral blood B. proportion of CXCR5+ CD4 metacluster 9. (\*p<0.05. \*\*\*p<0.001 Mann-Whitney)

In case of IgG myeloma, only patients with VGPR or better were included to avoid artifact of clonal Ig on total IgG level.